Plasma Science and Technology

PAPER

Dynamic dielectric recovery performance of serial vacuum and SF_6 gaps in HVDC interruption and its regulation method

To cite this article: Xian CHENG *et al* 2019 *Plasma Sci. Technol.* **21** 074010

Plasma Sci. Technol. **21** (2019) 074010 (7pp) https://doi.org/10.1088/2058-6272/ab1720

Dynamic dielectric recovery performance of serial vacuum and SF_6 gaps in HVDC interruption and its regulation method

Xian CHENG (程显)[1,2], **Peiyuan YANG** (杨培远)[1,2], **Guowei GE** (葛国伟)[1,2], **Qiliang WU** (吴启亮)[1] **and Wei XIE** (谢伟)[1,3]

[1] School of Electrical Engineering, Zhengzhou University, Zhengzhou 450001, People's Republic of China
[2] Henan Engineering Research Center of Power Transmission & Distribution Equipment and Electrical Insulation, Zhengzhou 450001, People's Republic of China
[3] Electric Power Research Institute, State Grid Henan Electric Power Company, Zhengzhou 450001, People's Republic of China

E-mail: ggw@dlut.edu.cn

Received 13 November 2018, revised 2 April 2019
Accepted for publication 8 April 2019
Published 20 May 2019

Abstract

Vacuum gaps have rapid dynamic dielectric recovery speed while SF_6 gaps have high insulation strength. The series-connected vacuum and SF_6 gaps are used as the main switch (MS), which combines their advantages. The work aims to verify the feasibility of serial vacuum and SF_6 gaps in mechanical HVDC interruption. The test circuit of the dynamic dielectric recovery performance (DDRP) is set up. The DDRP is tested under free recovery condition by the high voltage pulse source. The DDRP of the vacuum circuit breaker (VCB) and SF_6 gas circuit breaker (GCB) in DC interruption with active current injection is analyzed and compared. The test results indicate that the dielectric recovery duration of the VCB is below 30 μs while that of the GCB is above 100 μs. In order to achieve the cooperation between the VCB and GCB, a novel hybrid HVDC circuit breaker (CB) based on series-connected vacuum and SF_6 gaps is proposed. The 'voltage-zero' duration is created by introducing the follow current loop and there more recovery time for the dielectric recovery of the MS. The voltage distribution is controlled by the voltage dividing method so that the VCB undertakes the initial transient recovery voltage (TRV) and the later TRV is took by the GCB. The theoretical synergy characteristic of the novel HVDC CB is obtained. The paper supplies a new method to improve the custom mechanical HVDC CB, which is useful to achieve the HVDC CB with less serial breaks.

Keywords: dielectric recovery performance, vacuum interrupters, SF_6 interrupters

(Some figures may appear in colour only in the online journal)

1. Introduction

With the development of the distributed power supply, the multi-terminal HVDC transmission system is a future trend. There are a series of key technical problems to be solved for the HVDC application. The HVDC circuit breaker, which is one of the important key challenges, is used to connect and protect the multi-terminal HVDC system [1, 2].

The HVDC circuit breaker (CB) has been the research hotspot in the world. Common classification includes a mechanical type with active current injection, hybrid type with mechanical switch (MS) and power electronic equipment, high voltage power electronic apparatus type. The cost of the mechanical HVDC CB is low while that of the power electronic HVDC CB is high. The on state resistance of the power electronic HVDC CB is larger than that of the mechanical type. The hybrid HVDC CB combines the advantages of the MS and power electronic device, which has made significant progress in recent years [3]. The ABB Company designs the hybrid DC CB, whose rated voltage and

breaking current are 80 kV and 16 kA respectively. The breaking time is only 5 ms and it can be connected in series to achieve the 320 kV HVDC CB [4]. The 120 kV/7.5 kA HVDC CB prototype is designed by Alston Company [5]. China Global Interconnection Research Institute develops the 200 kV hybrid HVDC CB with the breaking current and time of 12 kA and 3 ms, respectively [6]. The mechanical HVDC CB with the active current injection is one of the main research directions of the HVDC CB. The dielectric recovery time of the vacuum is always below tens of microseconds. The MS is always a vacuum circuit breaker (VCB) driven by the high speed repulsion actuator. There are some mechanical DC CB prototypes whose rated voltage is below 80 kV because of the saturation effect of the long vacuum gap [7, 8]. The existing mechanical DC CB module includes 80 kV/10.5 kA/5 ms and 55 kV/16 kA/5 ms, which can be connected in a series to gain the mechanical HVDC CB. In 2018, the mechanical HVDC CB with the rated voltage of 160 kV has been designed and applied in the China Southern Power Grid [9, 10]. The on state resistance and cost of the mechanical HVDC are low while the synchronism and the serial structure of the HVDC CB are complex. As the development of the mechanical HVDC CB, the reliability and breaking speed will be enhanced.

The rated voltage of the commercial single-break VCB is below 72.5 kV in AC power system. In order to achieve the high voltage CB, multi-break VCBs is proposed by connecting single-break VCBs in series with grading capacitors. The MS of the mechanical HVDC CB is also multi-break VCBs. More serial breaks for the 800 kV HVDC CB are needed. The serial vacuum and SF_6 gaps has been proposed to combine the rapid dynamic dielectric recovery speed (DDRS) of the VCB and the high insulation strength of the GCB. In our previous research, the synergy cooperation and voltage distribution of the serial VCB and GCB have been investigated and we designed the fiber controlled AC prototype [11–13]. The vacuum gaps can be used to undertake the initial transient recovery voltage (TRV), which creates beneficial conditions for GCB so that it can improve the breaking capacity [14]. The first mechanical HVDC based on the serial VCB and GCB is proposed by S. Yanabu. The voltage distribution is adjusted by the nonlinear resistors and dividing resistors. The 250 kV/1.2 kA mechanical HVDC CB is achieved with the serial VCB and GCB [15]. Our team has established the custom mechanical HVDC CB simulation model and analyzed the dynamic voltage cooperation between the VCB and GCB [16]. The advantage of the mechanical HVDC CB based on serial VCB and GCB is that the number of series-connected breaks is less. However, the synergy mechanism and regulation methods of the above mechanical HVDC CB, according to the dynamic dielectric recovery performance (DDRP) of the vacuum and SF_6 gaps, are not clear [17].

In this work, the DDRP test circuit is designed with DC interruption current source and pulse high voltage source. The DDRP of the VCB and GCB in different arcing time, $\mathrm{d}i/\mathrm{d}t$ is obtained under free recovery condition. The DDRS time of the above arc-extinguishing medium is gained, which is very useful to the synergy control method in mechanical hybrid HVDC circuit breakers. The voltage-zero duration and voltage dividing method are introduced to the custom mechanical HVDC CB and the structure of the novel HVDC CB based on serial VCB and GCB is proposed. The effect of the regulation method is compared by simulation according to the DDRP data of each break. The test and simulation results verify the effectiveness of the novel structure, which is useful for high voltage applications.

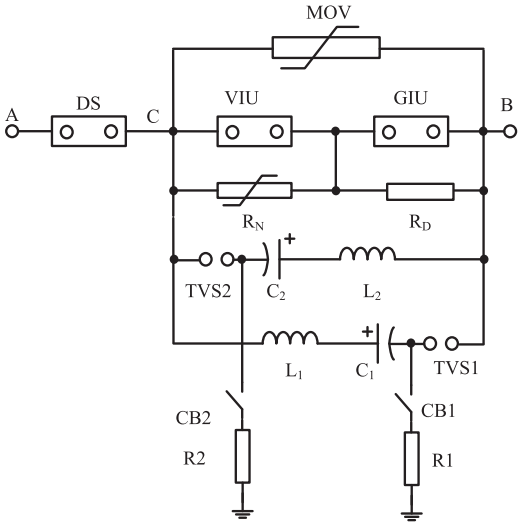

Figure 1. Schematic diagram of the mechanical HVDC CB based on serial VCB and GCB.

2. The mechanical HVDC circuit breakers based on serial VCB and GCB

The mechanical HVDC CB based on series-connected VCB and GCB is shown in figure 1. The vacuum interrupter unit (VIU) and SF_6 gas interrupter unit (GIU) are connected in a series, which are used as the MS of the mechanical HVDC CB. The voltage distribution between the VIU and GIU is controlled by the dividing resistors R_D and nonlinear resistors R_N. The resistance of R_N is much larger that of R_D when the nonlinear resistors do not act so that the initial TRV is almost endured by the VCB. After the nonlinear resistors act, the voltage of the VCB remains constant, which is dependent on the reference of the nonlinear resistor. The later TRV will be taken by the GIU. The oscillating current is produced by the positive current injection circuit L_2, C_2 and TVS_2 or negative current injection circuit L_1, C_1 and TVS_1. The metal oxide varistor (MOV) is the energy absorption unit. The disconnect switch (DS) is used to achieve the insulation after DC interruption. In this paper, we define the positive fault current as being from left to right. We only analyze the positive fault current interruption process.

As shown in figure 2, the interruption process of the mechanical HVDC based on serial VCB and GCB is as follows. I_{HCB}, I_C and I_S represent the total current, oscillating current and current of the MS. The total voltage, voltage of the VCB and GCB are described by V_{HCB}, V_{VI} and V_{GI} respectively. The

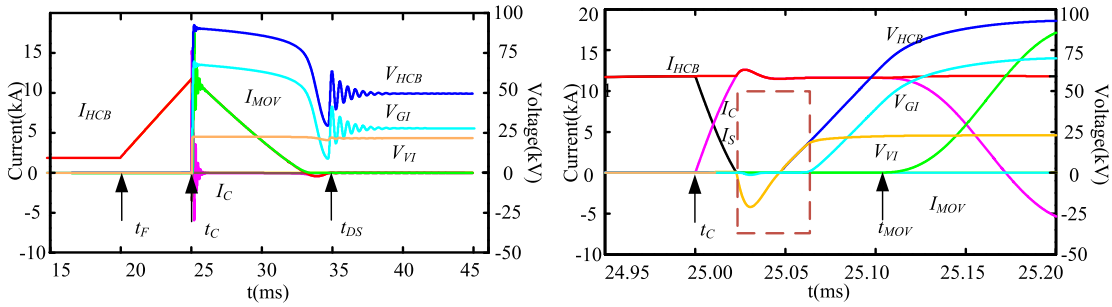

(a) The whole interruption waveform (b) The partial enlarged diagram of current zero region

Figure 2. Principle of the mechanical HVDC CB based on serial VCB and GCB.

normal rated current is 2 kA and starts to increase after the fault occurs at t_F. Then, the MS opens and the positive oscillating current circuit is closed by triggering TVS_2 when the opening distance of the MS is enough to break the current. The current of MS starts to decrease to zero after the introduction of the oscillating current. The arc of the serial VCB and GCB will be extinguished at current zero of the MS. The reserve TRV will be produced just after the current zero. The peak value of the reserve TRV is lower than the reference of the nonlinear resistors so that it is mainly undertaken by the VCB. After several microseconds, the positive TRV is produced and the initial positive TRV is also mainly endured by the VCB, which creates more recovery time for the GCB. The later positive TRV is taken by the GCB while the voltage of the VCB is constant, which is consistent to the reference voltage of R_N. The surge arresters MOV will act when the TRV reaches the threshold voltage and the energy will be absorbed by the MOV. The DC interruption process is finished after the DS interrupts the residual current.

The partial enlarged diagram of the current zero region is shown in figure 2(b). According to the above analysis, the current zero of the MS is created by introducing the reverse oscillating current. Then the TRV is produced and the voltage distribution between the VCB and GCB is dependent on the resistance relationship between the voltage dividing resistor and the nonlinear resistor. The dynamic dielectric recovery time of the VCB is always below 20 μs while the DDR time of the GCB may be above 100 μs. There is the synergy cooperation between the DDR and the voltage distribution of VCB and GCB. The VCB takes the initial TRV, which supplies about 50 μs for the DDR of the GCB, and then the GCB can endure the later TRV. In addition, the insulation of the GCB is linearly increasing with the gap length and pressure so that the static breakdown voltage of the GCB is higher than VCB [18–20]. The synergy strategy mainly depended on the DDRP of the VCB and GCB. We obtained the DDRP in DC interruption by experimental research.

3. The DDRP of the vacuum and SF_6 in DC interruption

3.1. Test circuit and configuration

The test circuit of the DDRP under free recovery condition is shown in figure 3. L_i and C_i represent the equivalent

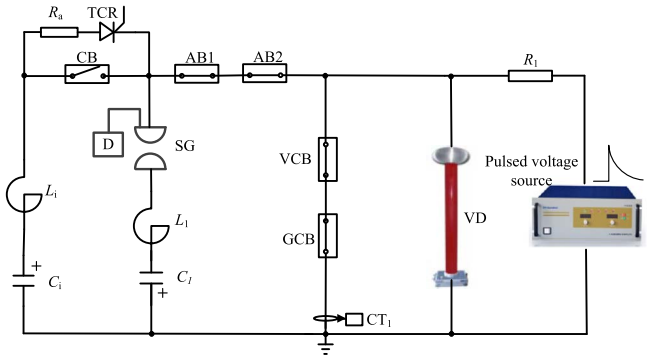

Figure 3. The test circuit of DDRP of VCB and GCB.

capacitance and inductance of the large current source while the reverse oscillating current circuit is composed of L_1, C_1 and SG. The auxiliary current circuit consists of TCR and R_a, which supplied the holding current for AB1 and AB2. The main power-frequency current will be introduced after the closing circuit breaker CB is closed. The reserve oscillating current is superposed into the main current and the DC interruption current can be produced. The protection switch is double-break VCBs by connecting AB1 and AB2 in series, which are used to achieve the insulation of the pulse high voltage. The rated current and voltage of AB are 20 kV and 1200 A respectively. The pulse voltage is triggered with a duration after the forced current zero. The peak value of the main current is 10 kA and the di/dt of the reverse currents are 13.3 A μs^{-1}, 22 A μs^{-1} and 30 A μs^{-1}, which are adjusted by changing the inductor L_1. The peak value and rising time of the pulse voltage source are 65 kV and 1.2 μs, respectively.

The principle of the DDRP test circuit is shown in figure 4. In the initial status, AB1, AB2, VCB and GCB are closed while TCR, CB, SG are open. The C_i is charged with positive voltage while the C_1 is charged with negative voltage. The auxiliary current is introduced by close TCR and the current is limited by the resistor R_a. The maximum value of the auxiliary current is about 50 A. Then the protection switches AB open and the auxiliary current supplies the holding current. The main current is introduced after the CB is closed. The contact resistance of CB is much less than that of the auxiliary current circuit. The test circuit break, such as VCB or GCB, opens with different arcing time. The reserve oscillating current circuit is superposed into the main current

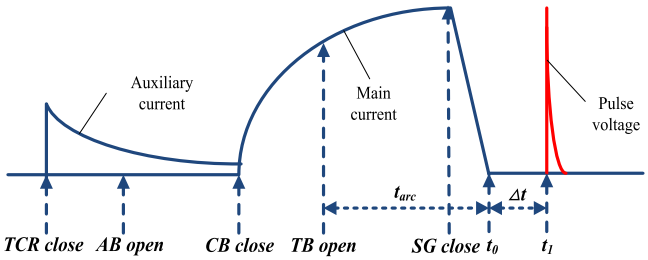

Figure 4. Principle of the DDRP test circuit.

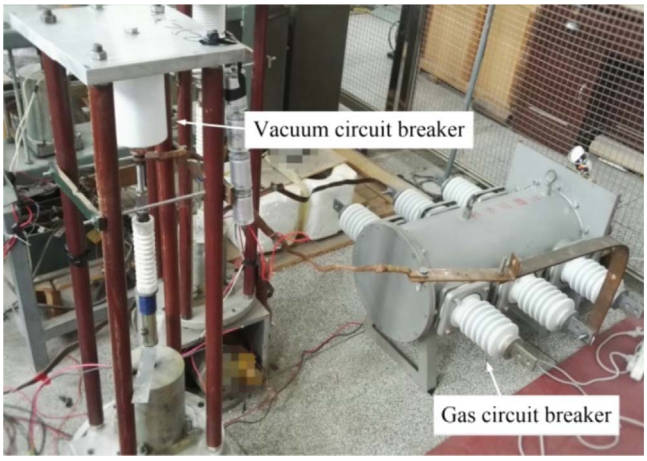

Figure 5. Prototype of the VCB and GCB.

after the SG is ignited. The forced current zero is created at t_0. The current flowed through the test circuit breakers (serial VCB and GCB) is the DC interruption current, which is the same to the current in mechanical DC CB breaking. The pulse voltage is triggered with a delay duration after the forced current zero. We can obtain the breakdown voltage in different delay durations when the main current is the same so that the DDRP can be obtained with a series of tests. The control accuracy of forced current zero and the moment of pulse voltage is vital to gain the effective results. The scatter of SG and pulse voltage is 10 μs and 5 μs, respectively, which ensure the accuracy of the test.

3.2. Results of dielectric recovery performance

The DDRP of the VCB and GCB in DC interruption is tested under the free recovery condition. The arcing time is adjusted from 3 ms to 7 ms for VCB while that of the GCB is adjusted from 5 ms to 18 ms. The maximum value of the main is 4 kA. The $\mathrm{d}i/\mathrm{d}t$ can be adjusted by changing the inductor of the reverse oscillating current circuit, which is 13.3 A $\mu\mathrm{s}^{-1}$, 22 A $\mu\mathrm{s}^{-1}$ and 30 A $\mu\mathrm{s}^{-1}$ in the test research.

The prototype of the VCB and GCB is shown in figure 5. The rated voltage is 10 kV while the breaking current is 20 kA. The permanent magnet actuator (PMA) is used to drive the VCB and the average opening speed is about 1.0 m s^{-1}. The structure of the GCB is magnetic arc control type and its breaking capacity is 10 kV/6.3 kA. The GCB is driven by the spring mechanism and the average opening speed is 2.5 m s^{-1}.

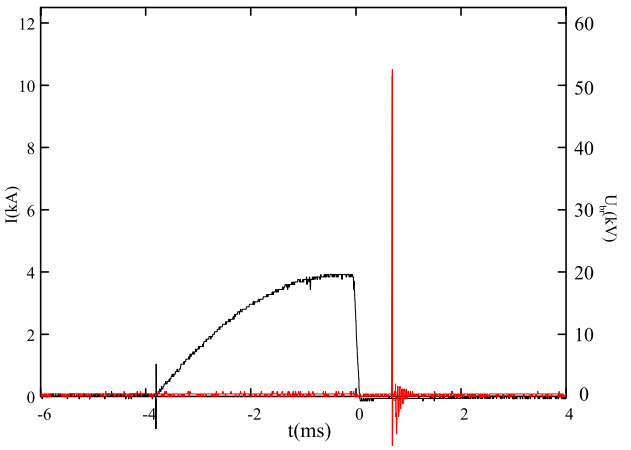

Figure 6. Typical breakdown in DDRP test.

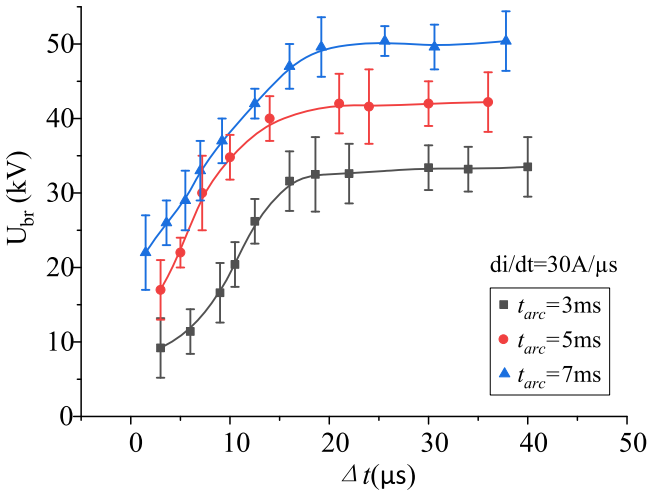

Figure 7. DDRP of VCB in different arcing time when the $\mathrm{d}i/\mathrm{d}t$ is 30 A $\mu\mathrm{s}^{-1}$.

The typical test waveform of the DDRP test is shown in figure 6. The peak value of the main current is 4 kA, the pulse voltage is applied after the forced current zero about 600 μs. The breakdown voltage is the DDR strength. The DDRP can be obtained by a lot of repeated tests in different delay durations.

3.2.1. DDRP of the VCB. When the peak value of the main current is 4 kA, the arcing time is 3 ms, 5 ms and 7 ms; the repeated tests are conducted in different delay durations. The DDRP of the VCB when the $\mathrm{d}i/\mathrm{d}t$ is 30 A $\mu\mathrm{s}^{-1}$ is obtained, which is shown in figure 7. The DDRS increases as the delay duration increases. The DDR time of VCB increases while the final DDRS decreases with decreasing arcing time. The initial DDRP of the VCB when the arcing time is 5 ms and 7 ms is almost the same. However, the final DDRS is higher when the arcing time is 7 ms because the final vacuum gap is longer than that of 5 ms. According to the figure 4, the DDR time of the VCB is below 30 μs and the insulation strength is about 50 kV when the arcing time is 7 ms. The vacuum gaps are 3 mm, 5 mm and 7 mm when the arcing time is 3 ms, 5 ms

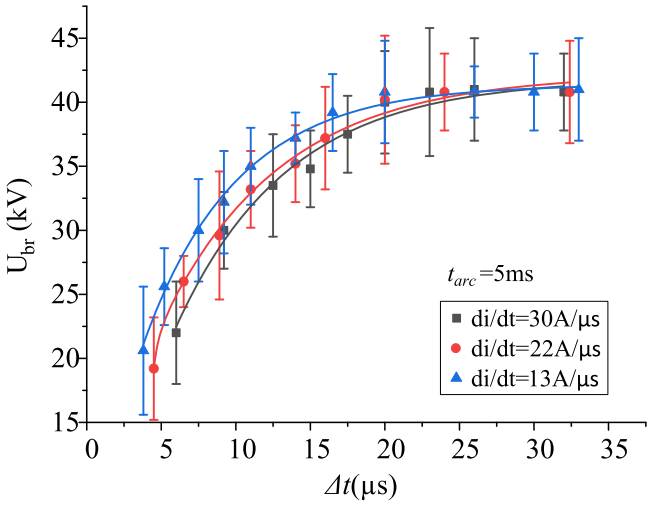

Figure 8. DDRP of VCB with different di/dt.

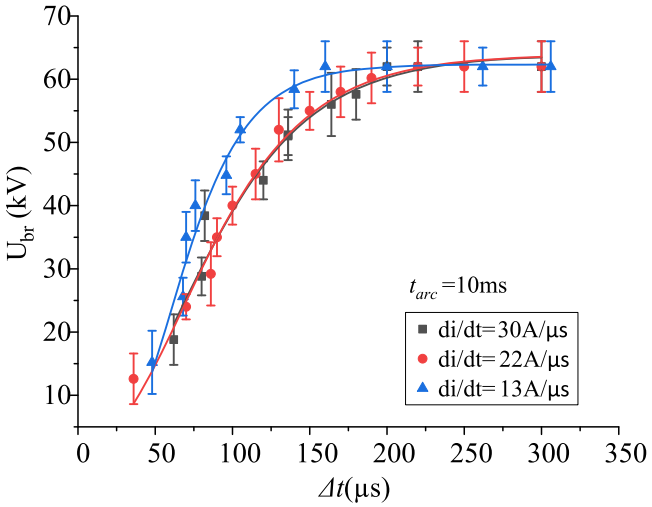

Figure 10. DDRP of GCB with different di/dt.

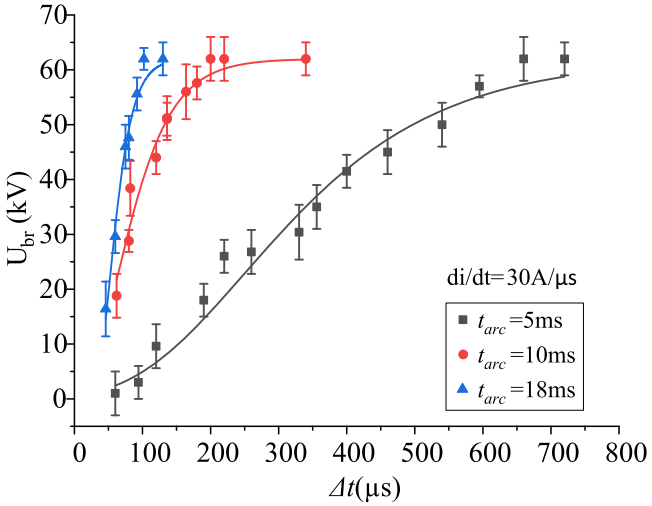

Figure 9. DDRP of GCB in different arcing time when the di/dt is 30 A μs^{-1}.

and 7 ms respectively. The optimal distance of the vacuum gap is 5–7 mm.

The DDRP of the VCB with different di/dt can be gained by the above repeated tests when the arcing time is 5 ms. The influence of the di/dt on the DDRP is shown in figure 8. When the di/dt is adjusted from 13.3 A μs^{-1} to 30 A μs^{-1}, as the di/dt increase, there is a slight decrease of the DDRP. The influence of the di/dt is not obvious. In the mechanical HVDC interruption, the frequency of the reserve oscillating current is always about 1–5 kHz. The oscillating frequency is 5 kHz in the test. Therefore, the influence of di/dt is ignored in the serial connection as the reserve oscillating current is the same.

3.2.2. DDRP of the GCB. The DDRP of the GCB is gained when the arcing time is 5 ms, 10 ms and 18 ms. DDRP in different arcing times are shown in figure 9. The DDR speed noticeably increases as the arcing time increases. The DDR time is above 600 μs when the arcing time is 5 ms and when it is below 100 μs when the arcing time is 18 ms. Generally, the arc extinguishing type is puffer type in GCB while the test GCB is magnetic arc blow type. The DDRP of the GCB with magnetic arc blow is lower than that of the puffer type GCB. The SF_6 gaps are 12.5 mm, 25 mm and 45 mm when the arcing time is 5 ms, 10 ms and 18 ms, respectively. According to test results, if we want to gain the advanced DDRP, the magnetic arc blow type GCB should be driven with high speed operation so that the contact distance can endure the transient interruption voltage (TIV).

The influence of the di/dt on the DDRP of the GCB is conducted when the arcing time is 10 ms. The influence of the di/dt on the DDRP is shown in figure 10. There is a great improvement of the DDRP with the arcing time of 5 ms, while the influence of the di/dt is slight if the arcing time is above 10 ms. The results indicate that the DDRP can be markedly enhanced by increasing the opening speed.

Based on the above DDRP results of the VCB and GCB, the DDR speed of the VCB is rapid and the DDR time is below 30 μs while the DDR time of the GCB is about 100 μs when the arcing time is 18 ms. The dynamic dielectric recovery strength (DDRS) of the GCB is larger than that of the VCB. The arcing time of the VCB should be between 5 ms and 7 ms, so that the DDR time is below 15 μs and the DDRS is above 50 kV. The arcing time can be represented by the contact distance. The average speeds of the VCB and GCB are 1.0 m s^{-1} and 2.5 m s^{-1}, respectively. So the best contact distance of the VCB should be 5–7 mm while the contact distance of the GCB should be above 25 mm. The maximum DDRS of the GCB is above 65 kV.

3.2.3. DDRP of the HCB. Based on the above results, the maximum DDRP of the HCB can be gained when the voltage distribution is consistent to the DDRP of each gap. The maximum DDRP of the HCB is shown in figure 11, when the vacuum gap and SF_6 gap are 5 mm and 25 mm, respectively. The DDRS increases as the delay duration Δt

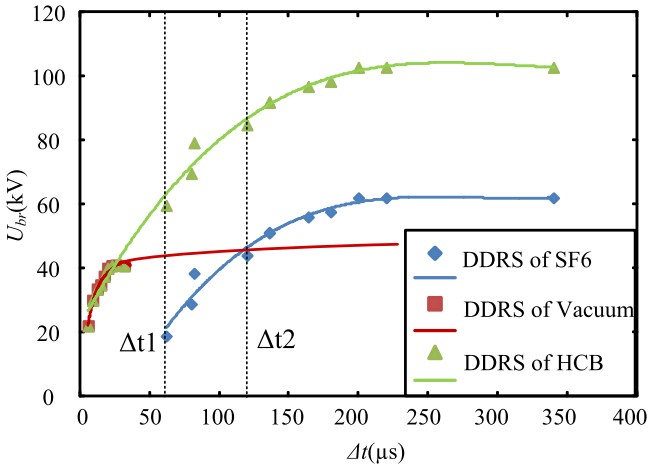

Figure 11. The maximum DDRP of the HCB.

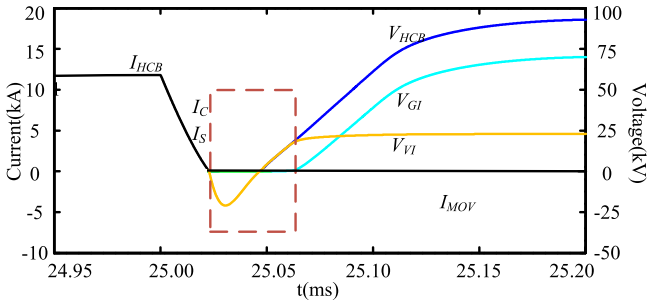

Figure 12. Current and voltage waveforms of the MS.

increases and the final DDRS can be above 105 kV when Δt is 200 μs.

4. The regulation of the serial vacuum and SF_6 gaps

4.1. Voltage distribution regulation

The voltage distribution of the serial VCB and GCB is dependent on the dividing resistor R_D and the nonlinear resistors R_N. According to the analysis in section 2, the initial TRV is mostly taken by the VCB while the GCB endures the later TRV. The current and voltage waveforms of the serial VCB and GCB in HVDC interruption are shown in figure 12. The test results in section 3 show that the DDR time of the VCB and GCB is about 10–30 μs and 200 μs with the final breakdown voltage of 50 kV and 65 kV respectively. The VCB can undertake the initial TRV until the value of the TRV reaches to 50 kV in 30 μs. However, the GCB can absolutely recover after 200 μs, so that there is blank region in the synergy cooperation between VCB and GCB. The maximum DDRP cannot be obtained by voltage distribution regulation.

4.2. Voltage-zero regulation

In order to create more recovery time for the MS, the follow current circuit is used to conduct the reverse TRV and then there will be a voltage-zero region in the reverse TRV state.

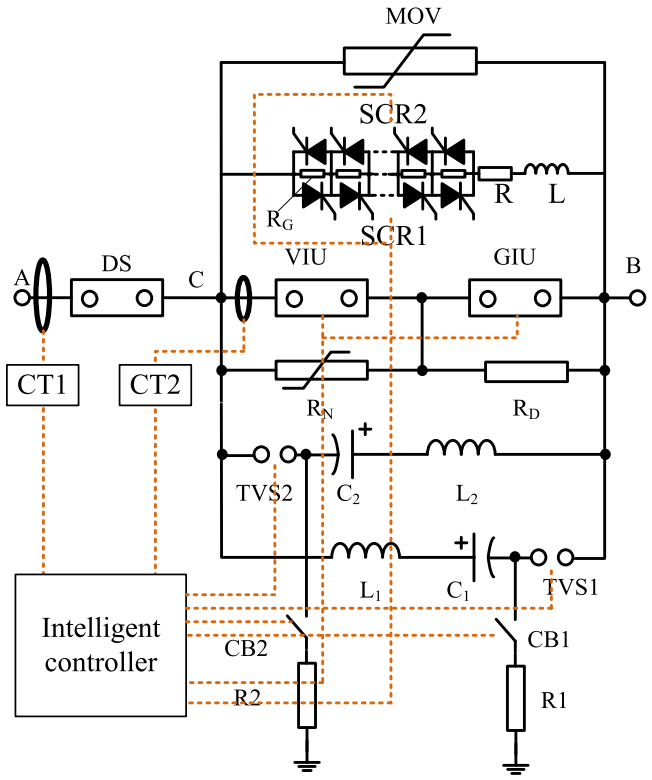

Figure 13. The novel mechanical HVDC CB with voltage-zero regulation.

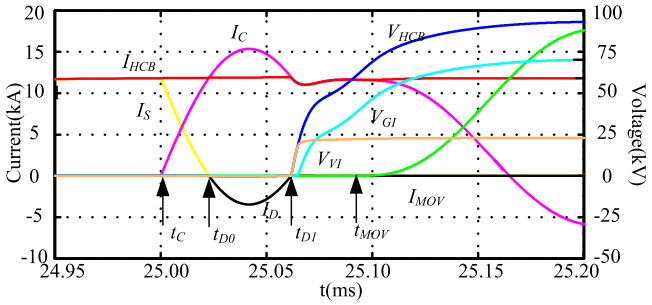

Figure 14. Interruption process of the novel hybrid HVDC CB at current zero region.

The serial positive SCR1 and negative SCR2 with current limiting resistor and inductor are used as the follow current circuit, which is connected to the MS in parallel. The novel mechanical HVDC CB with voltage-zero regulation is shown in figure 13. The current-limiting resistor R and reactor L are serially connected to the SCR, which are used to limit the maximum current of the follow current circuit. The positive SCR2 is cooperated with positive oscillating current circuit.

The interruption process of the novel HVDC CB with voltage-zero regulation at current zero region is shown in figure 14. There is no reserve TRV after the current zero of MS because the reserve TRV flows through the follow current circuit. The 'voltage-zero' region is achieved at the reserve TRV duration, which is from t_{D1} to t_{D2}. The positive SCR2 cut off after t_{D2} and the positive TRV is applied to the MS. Then the positive TRV distribution is adjusted by the

voltage-dividing regulation methods. The 'voltage-zero' duration created by the follow current circuit can supply more DDR time for the serial VCB and GCB, which is useful to gain the synergy cooperation of the DDRP of the VCB and GCB. The 'voltage zero' duration in the novel hybrid HVDC CB is arranged from several microseconds to hundred of microseconds by adjusting the oscillating frequency of the reverse current. If the voltage zero duration is greater than 200 μs, the serial VCB and GCB can be fully recovered. The calculated DDRS is above 105 kV based on the DDRP in figure 11. In addition, the VCB endures the initial TRV because it is full-recovery in 30 μs, and then the GCB takes over the later TRV. The above synergy cooperation can also supply the DDR time for about ten microseconds for GCB. Therefore, the novel hybrid HVDC CB can create the 'voltage-zero' duration to improve the DDRP of the MS in HVDC interruption. The prototype design and parameter optimization will be deeply investigated in future work.

5. Conclusion

The DDRP of the VCB and the GCB in DC interruption under free recovery condition is obtained. The influence of the arcing time and $\mathrm{d}i/\mathrm{d}t$ on the DDRP is obtained. The best arcing time of the VCB is 5–7 ms and the DDR time is below 15 μs. While the arcing time of the GCB should be above 18 ms so that the DDR time can be below 100 μs. The contact distance of the VCB should be 5–7 mm while that of the GCB should be above 36 mm.

According to the difference between the GCB and VCB, the voltage distribution and 'voltage-zero' regulation method are proposed to achieve the synergy cooperation between the VCB and GCB in DC interruption. The DDRS of the series-connected 10 kV VCB and GCB is above 105 kV when the voltage zero duration is above 200 μs.

The principle of the novel mechanical HVDC CB based on serial VCB and GCB is analyzed and tested. The DDRP of the serial VCB and GCB in DC interruption is obtained and the effectiveness of the novel mechanical HVDC CB is preliminarily verified, which provides the reference for future design.

Acknowledgments

This work was supported by National Natural Science Foundation of China (Nos. 51407163, 51777025), National Rail Transportation Electrification and Automation Engineering Technology Research Center (No. NEEC-2017B07), and China Postdoctoral Science Foundation (No. 2017M622370). Key scientific research projects of colleges and universities in Henan (16A470014, 19A470008).

ORCID iDs

Guowei GE (葛国伟) https://orcid.org/0000-0002-1740-7750

References

[1] International Council on Large Electric Systems (CIGRE) 2017 *CIGRE JWG A3/B4.34: Technical Requirements and Specifications of State-of-the-Art HVDC Switching Equipment* (Paris: CIGRE)
[2] Jiang Y and Wu J W 2016 *Plasma Sci. Technol.* **18** 311
[3] Callavik M *et al* 2012 *The hybrid HVDC breaker Technical paper Nov'2012* (Beijing: ABB Jiangjin Turbo Systems Co., Ltd)
[4] Hafner J 2011 *Proactive Hybrid HVDC Breakers-A Key Innovation for Reliable HVDC Grids Proc.* (Bologna: CIGRE Bologna Symposium) 2011, 1–8
[5] Grieshaber W *et al* 2014 Development and test of a 120 kV direct current circuit breaker *Proc. CIGRE Session Paris* (France: CIGRE) 1
[6] Wei X G *et al* 2013 *Autom. Electr. Power Syst.* **37** 95 (in Chinese)
[7] Tahata K *et al* 2015 HVDC circuit breaker for HVDC grid applications *Proc. 11th IET Int. Conf. on AC and DC Power Transmission Morehouse Lane Red Hook* (New York: Curran Associates, Inc.) 44
[8] Shao T *et al* 2014 *Appl. Phys. Lett.* **105** 071607
[9] Zhang Y K *et al* 2016 Experimental investigation on HVDC vacuum circuit breaker based on artificial current zero *Proc. 27th Int. Symp. on Discharges and Electrical Insulation in Vacuum (Suzhou, China, 18–23 September 2016)* 1
[10] Pan Y *et al* 2018 *Proc. Chin. Soc. Electr. Eng.* **38** 7113 (in Chinese)
[11] Cheng X *et al* 2017 *IEEE Trans. Plasma Sci.* **45** 2885
[12] Chen Z Q *et al* 2016 Simulation on the high current interruption principle for hybrid circuit breaker of vacuum interrupter and CO_2 gas interrupter *Proc. 27th Int. Symp. on Discharges and Electrical Insulation in Vacuum (Suzhou, China, 18–23 September 2016)* 1
[13] Cheng X *et al* 2013 *Plasma Sci. Technol.* **15** 800
[14] Smeets R P P *et al* 2007 *IEEE Trans. Plasma Sci.* **35** 933
[15] Senda T *et al* 1984 *IEEE Trans. Power Appar. Syst.* **PAS-103** 545
[16] Ge G W *et al* 2013 HVDC hybrid circuit breaker based on SF6 interrupter and vacuum interrupter in series *Proc. 2nd Int. Conf. on Electric Power Equipment-Switching Technology (Matsue, Japan, 20–23 October 2013)* 1
[17] Lenz V 2015 *DC Current Breaking Solutions in HVDC Applications (Master Thesis) ETH Zürich*
[18] Shao T *et al* 2017 *IEEE Trans. Dielectr. Electr. Insul.* **24** 1557
[19] Shao T *et al* 2011 *Plasma Sci. Technol.* **13** 591
[20] Zhao X L, Yan J D and Xiao D M 2018 *Plasma Sci. Technol.* **20** 085404